

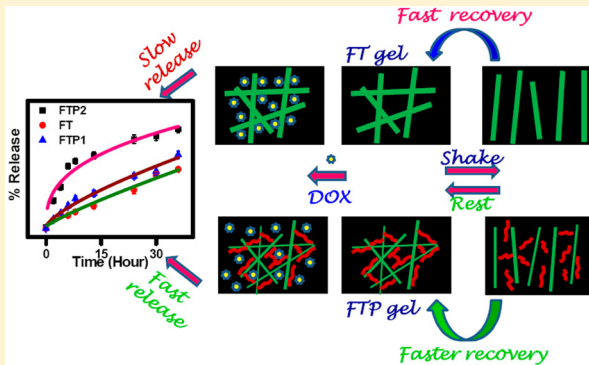
Integration of Poly(ethylene glycol) in N-Fluorenylmethoxycarbonyl-L-tryptophan Hydrogel Influencing Mechanical, Thixotropic, and Release Properties

Priyadarshi Chakraborty, Sanjoy Mondal, Subhankar Khara, Partha Bairi, and Arun K. Nandi*

Polymer Science Unit, Indian Association for the Cultivation of Science, Jadavpur Kolkata-700 032, India

Supporting Information

ABSTRACT: Polyethylene glycol (PEG) is incorporated to improve the mechanical properties of *N*-fluorenylmethoxycarbonyl-L-tryptophan (FT) hydrogel producing the hybrid (FTP) gels designated as FTP1, FTP2.5, etc. having PEG concentrations of 0.05 and 0.125% (w/v), respectively. Both the FT and FTP1 gels exhibit fibrillar network morphology; the fibers of the FTP1 gel are thinner than those of the FT gel. FTP gels exhibit a magnificent improvement in mechanical properties, and the storage and complex moduli increase with a maximum of ~2800% for the FTP2.5 gel. Creep recovery experiment exhibits a maximum strain recovery of 90% for the FTP1 gel. The thixotropic property is observed for both FT and FTP gels and the rate of recovery increases with increase of PEG concentration; the latter acts as a molecular adhesive to the gel fibers bringing back the network structure easily. Gelation of FT causes a 5-fold increase of fluorescence intensity due to molecular aggregation, and with increase of FT concentration the ratio of fluorescence intensities at 470 and 395 nm increases. Exploiting the thixotropic property of FT and FTP hybrid gels, doxorubicin (DOX) is successfully encapsulated, and tunable release of DOX using appropriate amount of PEG in the gel matrix under physiological conditions is observed.



INTRODUCTION

Low molecular weight gelators (LMWG) are organic molecules competent enough to gelatinize water and/or organic solvents at very low concentrations due to generation of three-dimensional entangled networks via different types of non-covalent interactions like H-bonding, $\pi-\pi$ stacking, etc.^{1–8} This kind of network formation is generated from the nucleation and subsequent growth of the fibers,^{9–12} and the entanglement occurs from its branching at the tips or at its side faces.¹³ Supramolecular hydrogels are endowed with excellent properties like thermoreversibility, stimuli responsiveness, and soft nature, making them suitable for applications in sensing, soft lithography,¹⁴ drug delivery,^{15–17} pollutant capture and release,^{18–20} templated nano materials synthesis,²¹ tissue engineering,^{22–24} and designing different microarray kits.²⁵ Although supramolecular gels possess plethora of advantages, their mechanical stability is limited as a small external mechanical force can overpower the weak intermolecular forces (H-bonding and $\pi-\pi$ stacking) holding the components together. On the other hand, polymers are mechanically stable and strong as they are comprised of the monomeric units joined by covalent bonds. The elegant combination of the mechanical stability and robustness of the polymers with the reversibility and external switchability of supramolecular systems may possibly give birth to a new generation of soft

materials with excellent mechanical stability still retaining the characteristics and advantages of supramolecular systems.^{26,27}

Peptide and amino acid based moieties behave as excellent candidates for hydrogelation as they self-assemble by non-covalent interactions in water including H-bonding, electrostatic, and $\pi-\pi$ interactions. Xu and co-workers have contributed significantly to functional supramolecular short peptide-based hydrogels with myriad applications including treatment of uranium-contaminated wounds, immobilizing enzymes to carry out catalytic reactions in organic solvents, as anti-inflammatory agents, enzyme inhibitor detection, etc.^{28–30} Hydrogelation by a short peptide, Fmoc-Phe-Phe (Fmoc: *N*-fluorenylmethoxycarbonyl; Phe: phenylalanine) showing remarkable mechanical properties is utilized for tissue engineering and regeneration due to its biocompatibility.³¹ Banerjee and co-workers have reported a hydrogel based on N-terminally Fmoc-protected amino acid, Fmoc-Phe-OH, which is also used to prepare and stabilize fluorescent silver nanoclusters.³²

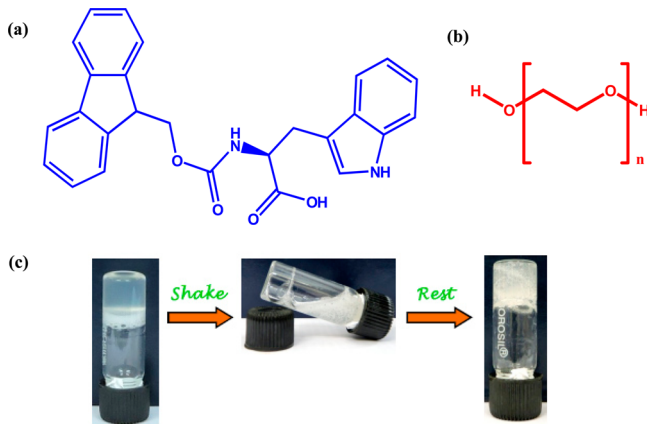
It would be very interesting if N-terminally Fmoc-protected tryptophan, containing an indole functional group (Scheme 1), can produce a supramolecular hydrogel. The carboxylic acid,

Received: March 12, 2015

Revised: April 17, 2015

Published: April 17, 2015

Scheme 1. Chemical Structures of (a) Fmoc-L-tryptophan and (b) Polyethylene Glycol (Wedge Indicates That the N Atom Is above the Plane) and (c) Schematic Representation of the Thixotropic Property of the FT Gel



amide, and secondary amine groups may be involved in the H-bonding process. Also both the indole and Fmoc groups can play important roles for the intermolecular $\pi-\pi$ interaction, which is also another prerequisite for gelation. Stimulated by this idea, we have produced a hydrogel of Fmoc protected L-tryptophan (FT) at pH 7, and we observe that the hydrogel is thixotropic in nature (Scheme 1) showing good strain recovery although it is mechanically weak. It would be very interesting to perceive whether we can improve its physical and mechanical properties by incorporating a biocompatible polymer, polyethylene glycol (PEG) (Scheme 1) in the FT hydrogels. Complimenting our expectation, the hybrid hydrogels thus obtained show much augmented and tunable storage and loss modulus values (G' and G''), improved strain recovery, and improved thixotropic behavior. The FT hydrogel also exhibits increased fluorescence intensity from its solution, which increases with the increase of gelator concentration and also increases with the addition of PEG up to a certain concentration. Possible explanations of the enhancement of physical, mechanical, and thixotropic properties are offered. Exploiting the thixotropic property of the gels along with the biocompatibility of the components, we have incorporated an anticancer drug doxorubicin (DOX) in the gel matrices, and, interestingly, the DOX release is tuned by the PEG concentration within the FT gel. The diffusion coefficient of the drug in the FT and hybrid gels have been computed to gain insight into the mechanism of the drug release from the hybrid gels. To the best of our knowledge this type of polymer-induced enhancement of thixotropy and drug release property of a supramolecular hydrogel is being reported for the first time.

■ EXPERIMENTAL SECTION

Materials. Fmoc-L-tryptophan (FT) and poly(ethylene glycol) (PEG) ($M_n = 4000$) were purchased from SRL, Mumbai, India. They were used as received. Buffer capsules of pH 7 were purchased from Merck, Mumbai, India. Water was double distilled before use.

Preparation of FT and FTP Hybrid Gels. The FT gel was prepared by dissolving the required quantity of FT in buffer solution of pH 7 at 70 °C in a capped tube (i.d. = 1.2 cm), followed by sonication for 3 min and it was then cooled to 30 °C producing an almost transparent gel. The gel formation was

recognized by the cessation of flow on inverting the tube. Minimum gelation concentration was found to be 0.2% (w/v). For convenience we used 0.4% (w/v) concentration of the gelator in all the experiments and this gel is designated as the FT gel throughout the manuscript, if not otherwise mentioned. For the preparation of the hybrid gels, at first a solution of PEG was prepared in pH 7 buffer having concentration 10 mg/mL. This solution was then used for making the hybrid gels. The hybrid gels are designated as FTP1, FTP1.5, FTP2, FTP2.5, FTP3, etc. according to the amount of polymer (mg) added into 2 mL of the FT solution during gelation, i.e., having PEG concentrations of 0.05, 0.075, 0.10, 0.125, 0.15% (w/v), respectively. In all these cases, the FT concentration was fixed (0.4% (w/v)). All the FT and FTP gels were thermoreversible in nature.

Microscopy. The morphologies of all the gels were investigated by transmission electron microscopy (TEM). Small portion of the FT gel and FTP1 hybrid gels were diluted and drop casted on carbon coated copper grid (300 mesh), and the samples were dried in open air at 30 °C. Finally, the samples were kept in vacuum for overnight before the experiment.

Thermal Study. The gel melting temperature of both the FT gel and FTP2 gels were determined using a differential scanning calorimeter (PerkinElmer, Diamond DSC). Before each set of experiments, the instrument was calibrated with indium. The FT and FTP2 gel samples were taken in large-volume capsules (LVC) fitted with O-rings and were equilibrated at 10 °C for 10 min. They were heated at the heating rate of 10 °C min⁻¹ to 90 °C under a nitrogen atmosphere. After that they were cooled at a rate of 5 °C min⁻¹ to 10 °C where they were kept for 30 min and were again heated at the rate of 10 °C min⁻¹. The peak position of the endotherm was taken as the melting point of the samples.

Spectroscopy. The UV-vis spectra of the samples were recorded with a Hewlett-Packard UV-vis spectrophotometer (model 8453) in a cuvette of 0.1 cm path length. Fluorescence study of the FT gels of different concentrations, FTP2, FTP3, and FTP4 gel were carried out in a Horiba Jobin Yvon Fluoromax 3 instrument. Each gel sample was prepared in a quartz cell of 1 cm path length and was excited at 265 nm. The emission scans were recorded from 285 to 600 nm using a slit width of 5 nm with a 1 nm wavelength increment having an integration time of 0.1 s. The FT-IR spectra of pure components and the xerogels were recorded using KBr pellets in a PerkinElmer FT-IR instrument (FT-IR-8400S).

Diffraction Study. Wide angle X-ray scattering (WAXS) experiments of pure FT powder, FT and FTP2 xerogels were performed in a Bruker AXS diffractometer (model D8 Advance) using a Lynx Eye detector. The instrument was operated at a 40 kV voltage and at a 40 mA current. Samples were placed on glass slides and were scanned in the range of $2\theta = 4-50^\circ$ at the scan rate of 0.5 s/step with a step width of 0.02°.

Rheology. To understand the mechanical property of the gels, rheological experiments were performed with an advanced rheometer (AR 2000, TA Instrument, USA) using cone plate geometry on a Peltier plate. The diameter of the plate was 40 mm and cone angle was 4° with a plate gap of 121 μ m. The G' (storage modulus) and G'' (loss modulus) values of the gels were calculated by taking the values at a particular frequency (2 rad/s) in the linear viscoelastic region of the G' , G'' versus angular frequency plots. The complex modulus (G^*) was calculated from the relation

$$G^* = (G^2 + G''^2)^{1/2} \quad (1)$$

Drug Loading and Drug Release Study. At first FT, FTP1, and FTP2 gels were prepared using methods described above. Then they were transformed to sol state by rigorous vortexing. A stock solution of DOX is prepared (0.6 mg/mL) in pH 7 buffer. Equal amounts (0.2 mL) of this DOX solution were added to the 2 mL sol of FT, FTP1, and FTP2 gels separately and the mixtures were vortexed again for homogeneous mixing. The thixotropic property helps in gelation of the mixture solutions by waiting for half an hour and thus forming the self-supported DOX encapsulated FT-DOX, FTP1-DOX, and FTP2-DOX hydrogels (Supporting Information Figure S1). Thus, we have elegantly used the thixotropic property to load DOX in the gels avoiding the heating procedure. To study the release of DOX from the FT-DOX, FTP1-DOX, and FTP2-DOX hydrogels, we poured 2 mL buffer solution (pH 7) gently on the top of the gels and placed them in a water bath thermostated at 37 °C. The stability of the gel when exposed to phosphate buffered saline (PBS) solution was more than 48 h. To study the time scale of DOX release from the hydrogels small aliquots (0.4 mL) of the buffer solution were taken for UV-vis spectroscopic studies at different time intervals, and the absorbance values at 490 nm were recorded in a repeated fashion (three times), and the average data are used for the calculation of percentage release of the drug. We have measured the DOX release up to 30 6 h.

■ RESULT AND DISCUSSION

Structural Analysis. Fourier transform infrared (FTIR) spectra of pure FT powder and FT and FTP2 xerogels are obtained to investigate the nature of interactions present in the FT gel state and also to comprehend the interactions between FT and PEG (Figure 1). The FTIR spectrum of FT powder

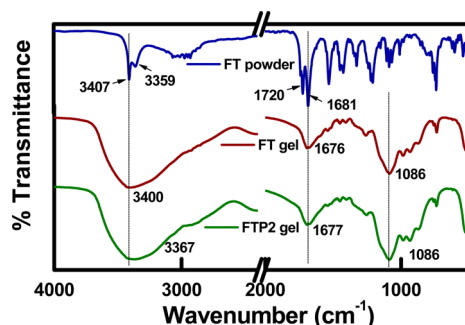


Figure 1. FTIR spectra of FT powder and FT and FTP2 xerogels.

exhibits two stretching peaks at 3407 and 3359 cm^{-1} due to $-\text{NH}$ vibrations of the secondary amine present in the indole ring and that of the amide group, respectively. In the FT gel, these peaks combine to form a broad peak at 3400 cm^{-1} , indicating the involvement of these groups in the intermolecular H-bonding process during gelation. In the FTP2 xerogel the broad peak is observed at 3367 cm^{-1} and this 33 cm^{-1} shift to lower frequency from that of the FT gel may be attributed to the H-bonding interactions between the $-\text{OH}$ groups of PEG with the $-\text{NH}$ -groups of indole ring and amide groups of FT. The two peaks at 1720 and 1681 cm^{-1} in the FT powder, attributed to the carbonyl stretching vibrations of the acid and amide groups, respectively,³³ exhibit a broad peak at 1676 cm^{-1} in the FT gel, indicating involvement in the

intermolecular H-bonding of $>\text{C}=\text{O}$ groups. After addition of PEG, this peak remains almost at the same position, which indicates that the extent of H-bonding remains the same whether the H atom comes from the FT molecule or from the $-\text{OH}$ groups of PEG. A number of peaks in the region 1320–1000 cm^{-1} are observed in the pure FT powder corresponding to the C–O groups present in the FT molecule. However, the FT gel exhibits a broad peak at 1086 cm^{-1} and this broadness also accounts for the H-bonding interactions present in the FT gel. This peak remains at the same position in the FTP2 gel, indicating the same extent of H-bonding. As a broad peak is already present in the vibrational region of ether groups and the concentration of PEG is very low compared to that of the gelator FT, the vibrational bands of ether groups of PEG are not visible in the FTIR spectra of FTP2 gel.

The WAXS patterns of FT powder and FT and FTP2 xerogels (Figure S2) indicate that FT powder displays a large number of sharp diffraction peaks, which are absent in FT and FTP2 xerogel. It suggests that the crystalline patterns of the FT powder are destroyed during gelation, and new ordered structure due to self-assembling of FT is produced in the gel. WAXS pattern of the FT xerogel shows two diffraction peaks at $2\theta = 16^\circ$ and 21° corresponding to the *d* spacings of 5.5 and 4.3 Å, respectively. The diffraction peak at $2\theta = 21^\circ$ corresponds to the $\pi-\pi$ stacking distance (4.3 Å) of FT xerogel.^{34,35} This diffraction peak is also present in the FTP2 xerogel, which surmises that the $\pi-\pi$ stacking interactions are also present in the FTP2 xerogel. However, the absence of the diffraction peak at $2\theta = 16^\circ$ in the FTP2 gel indicates some disorganization of the self-assembled structure due to the integration of PEG.

Morphology. Transmission electron microscopy (TEM) is performed to get insight into the morphology of the FT gel as well as to understand the change in the morphology of the gel after addition of PEG. Figure 2a,b and Figure S3 depict the TEM images of the FT and FTP1 xerogels, and it is evident from the figures that both the gels possess fibrillar network morphologies. However, it is interesting to observe that the fibers of the FTP1 gel are thinner than those of FT gel; also the network density is higher in the former than that of the later gel. The histograms of the fiber diameters are presented in Figure 2c,d. The calculated value of the average fiber diameter for the FT gel is 42.4 ± 10 nm, and that for the FTP1 gel is 14.6 ± 4.2 nm. So, with the addition of 1 mg PEG to the FT gel, the average fiber diameter decreases by ~28 nm. Also the average fiber density increases from $46/\mu\text{m}^2$ in FT gel to $75/\mu\text{m}^2$ in FTP1 gel, and the average junction density increases from $7/\mu\text{m}^2$ in FT gel to $13/\mu\text{m}^2$ in FTP1 gel. No definite reason for this observation is known, and a probable explanation may be given as follows.

The formation of FT and FTP gels are depicted in Scheme 2. FT molecules self-assemble via H-bonding and π -stacking interactions as evident from the FTIR and XRD spectra. The Fmoc and indole moieties are responsible for π -stacking process, and the amide, secondary amine, and carboxylic acid functional groups present in FT are involved in the H-bonding process. The lateral growth occurs through the H-bonding interactions, while the longitudinal growth occurs through both π -stacking and H-bonding interactions. A combination of both the lateral and longitudinal growths by self-assembling of the FT molecules generates fibrils which further grow both ways to produce the fibers. The tryptophan moiety is more hydrophilic than the Fmoc moiety, and it acts as H-bonding part as depicted in the scheme. Therefore, there would be a

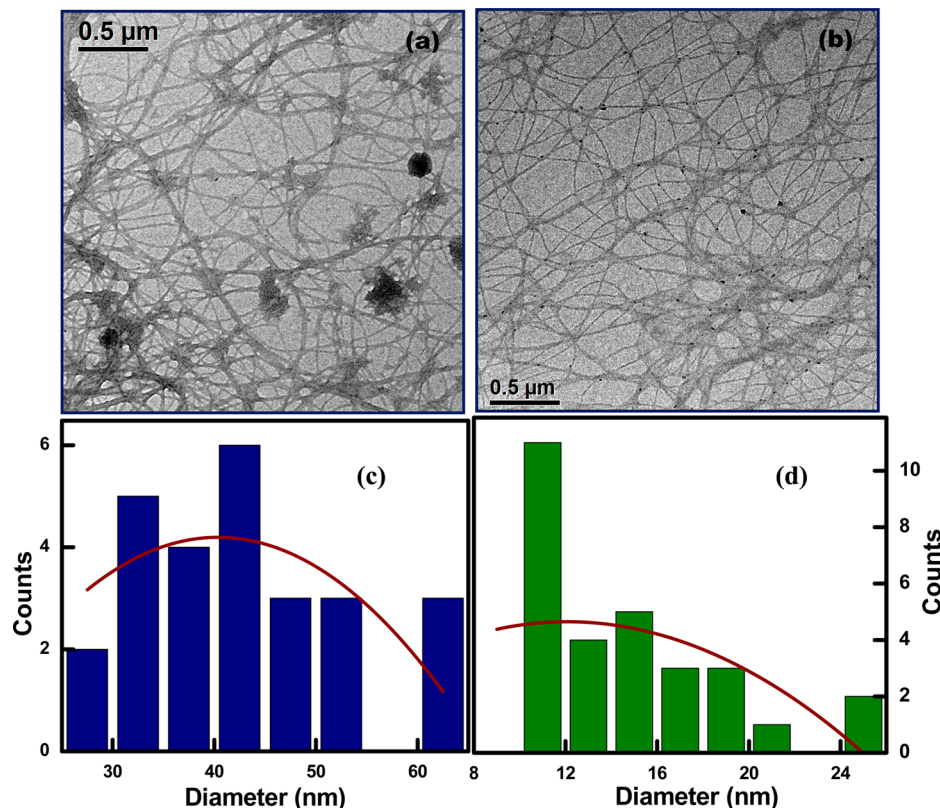
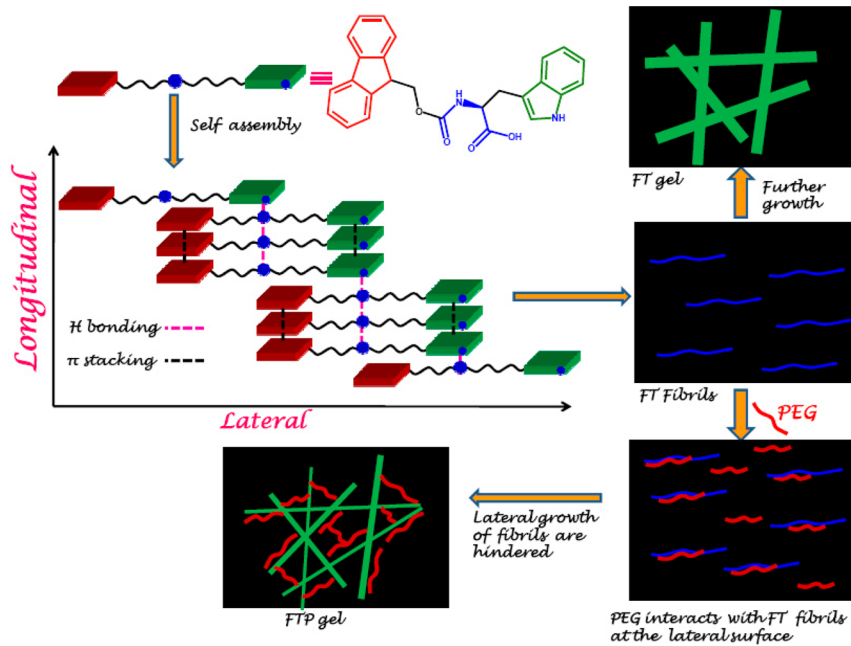


Figure 2. TEM images of (a) FT and (b) FTP1 xerogels. Histograms of the fiber diameters of (c) FT gel and (d) FTP1 gel.

Scheme 2. Schematic Representation of the Formation of FT Fibrils and Thinning of the Fibers by Addition of PEG



competition between intermolecular H-bonding of FT and that with water, but due to the complementary π -stacking of the Fmoc moiety of FT, the H-bonding of former type is more thermodynamically favorable than that with water molecules. As a result of the fiber formation, the tryptophan moiety prefers to remain at the fiber surface, whereas the Fmoc moiety forms the core of the fiber by π stacking process, which is also apparent from the scheme. A supporting evidence of it would

be discussed later from fluorescence results. Surface forces of the entangled fibers help to entrap a large amount of solvent (water) molecules producing the FT gel. When PEG is added to the system, interaction between FT and PEG occurs mainly at the lateral surface, and the lateral growth of FT fibers becomes hindered due to the crystallographic mismatch.²⁰ Hence the fibers of the FTP1 gel are thinner than that of the FT gel. The higher network density of FTP1 gel than that of

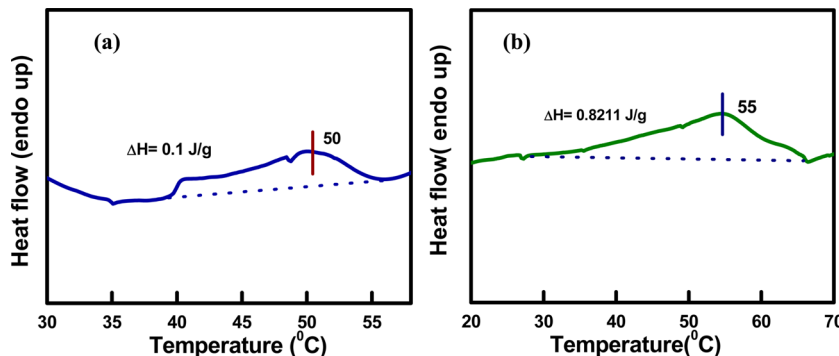


Figure 3. DSC thermograms of (a) FT gel at a concentration of 1.5% w/v and (b) FTP2 gel with the same FT concentration.

FT gel may be attributed to the PEG, which acts as an impurity at the growth front of the fibers causing protuberance and noncrystallographic branching of fibers occurs.³⁶ It also causes the increase of fiber density in the FTP1 gel.

Thermal Study. The gel melting temperatures are obtained from DSC measurements of the FT and FTP2 gels at a concentration of 1.5% (w/v) (Figure 3). In both the cases, a broad melting peak is observed due to the polydispersity of physical cross-links present in the gels. It is interesting to note that the melting temperature and enthalpy values are higher in the FTP2 gel (55 °C, $\Delta H = 0.8 \text{ J/g}$) than that of the FT gel (50 °C, $\Delta H = 0.1 \text{ J/g}$) indicating greater thermal stability of the FTP2 gel than that of the FT gel. The thermal effect depicted in Figure 3 occurs due to the breaking of supramolecular (physical) bonds present in the gel structures. In the presence of PEG, FT molecules enjoy supramolecular interactions not only with each other but also with PEG as evident from the lower energy (33 cm^{-1}) shift of the secondary amine and amide vibration peaks discussed earlier. This increases the number of physical bonds within the system, which in turn enhances the thermal stability of the FTP2 gels as manifested in the higher melting point and enthalpy data.

Mechanical Property. Rheological properties of the FT and the FTP gels with different concentrations of PEG are investigated to get an insight into the formation of the gel networks and also to understand the influence of PEG in the gel properties. Figure 4a shows the variation of storage and loss moduli with frequency for the FT, FTP1, and FTP2 gels. It is evident from the figure that in the three systems the variation of G' is almost invariant with frequency particularly at low frequency region and G' is much greater than G'' . These results characterize the systems to behave as a gel. Most important is that there is a significant increase of both the storage (G') and loss (G'') moduli values of the FTP1 and FTP2 gels relative to the FT gel. The storage modulus (G') indicates the amount of energy stored in the system, characterizing the solid like property of the gel and it increases significantly with the addition of PEG showing a maximum increase (2815%) for FTP2.5 gel than that of the FT gel. The loss modulus (G''), which indicates the amount of energy dissipated in the network, characterizing the liquid-like property of the gel, also increases almost in the same manner as G' with a maximum increase (2525%) for FTP2 gel (Table-S1). It may be attributed to the same reason for the dramatic increase of storage and loss modulus of the FTP gels. At higher frequency, the G' and G'' values are scattered, probably due to the rupturing of the gel network. The complex modulus (G^*), which is the ratio of stress to strain under vibratory conditions, also varies with

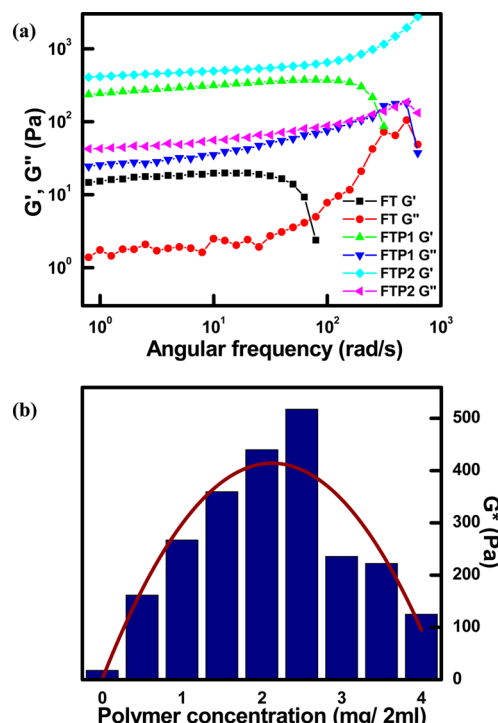


Figure 4. (a) Oscillation frequency dependency of modulus values (G' and G'') of FT, FTP1, and FTP2 gels. (b) The change in complex modulus value with the change in concentration of the polymer into 2 mL FT gel.

polymer concentration (Figure 4b, Table S1). It is evident from the figure that the G^* value initially increases with the addition of PEG in the FT gel showing a maximum increase (2811%) for FTP2.5 gel from that of FT gel. The decrease of G^* at higher concentrations of PEG (>2.5 mg) probably takes place because of the increased self-aggregation between the PEG chains rather than forming an assembly with FT molecules.²⁰ This type of increase of modulus values on addition of PEG may be ascribed to the formation of thinner (by ~ 28 nm) fibers with higher fiber density (by $29/\mu\text{m}^2$) and also with the increase of average junction density (by $6/\mu\text{m}^2$) than that of FT fibers. These factors help to entrap the water molecules more closely, with a greater amount of its surface force causing the storing or dissipation of the external mechanical energy more efficiently.

Figure 5a portrays the shear viscosity versus shear rate plots of FT, FTP1, and FTP2 gels. For all the three gels non-Newtonian viscosity is observed showing shear thinning

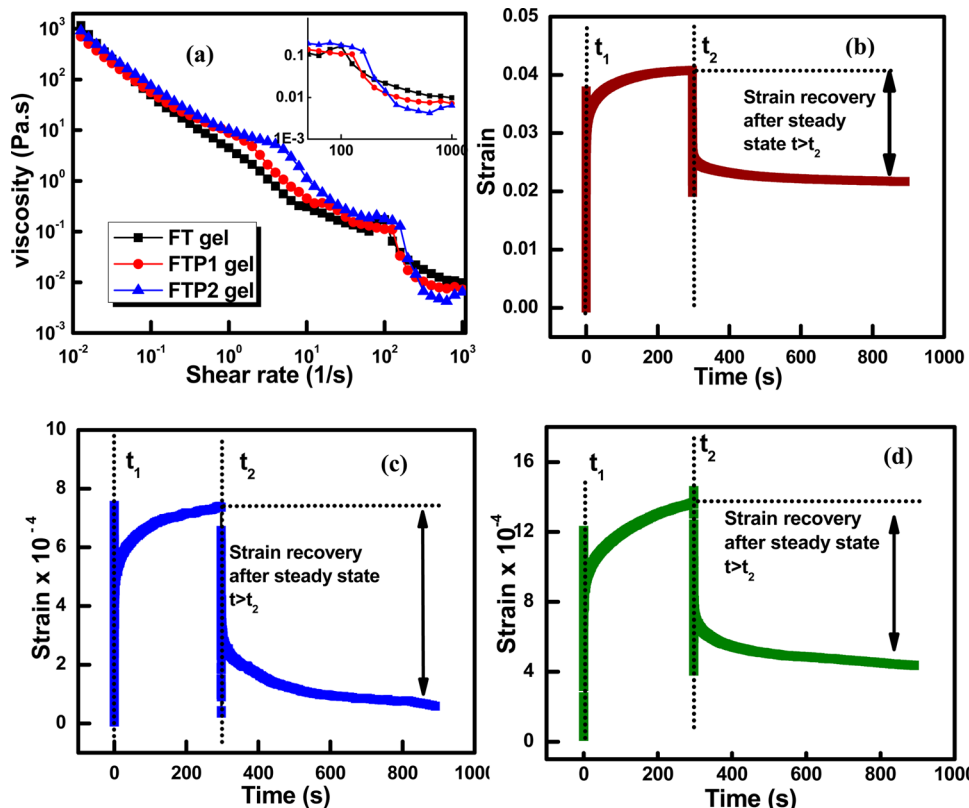


Figure 5. (a) Shear viscosity versus shear rate plot of FT, FTP1, and FTP2 gel at 25 °C. Stress relaxation as a function of time in the creep recovery investigated separately with (b) FT gel (c) FTP1 gel, and (d) FTP2 gel at applied stress of 0.5 Pa.

behavior throughout a particular shear rate region. However, there is a small increase of viscosity with increase of shear rate (i.e., shear thickening) at two intermediate shear rates, particularly for the FTP1 and FTP2 gels. Finally there is a sudden fall of viscosity in all cases, indicating the transformation of the gel into the sol state. No definite reason for this abnormal behavior of FT and FTP gels is known, and a probable reason may be that the applied shear rate causes the PEG coils to be straightened first and then H-bonding interaction with the FT fibrils increases, causing the shear thickening. However, on continuous applied shear rate, the entanglements of the FT fibers become destroyed, offering further H-bonding possibility with the PEG chains, showing the second shear thickening. It is important to note that the FT gel does not exhibit the first shear thickening, but it exhibits the second one, supporting the above explanation. Finally, at the higher shear rate, the physical cross-links of FT fibrils get disrupted, causing the gels to break. The critical shear rate values for the disruption (calculated from the inset of Figure 5a) are 100, 126, and 159 s⁻¹ for the FT, FTP1, and FTP2 gels, respectively, suggesting an increase of mechanical stability with respect to applied shear of the gel with the addition of PEG.

Viscoelasticity is a property that exhibits both viscous and elastic characteristics of the material when subjected to a deformation. Viscous materials resist shear flow and strain linearly with time on application of stress, and elastic materials exhibit strain when stretched and subsequent rapid recovery with time to the original state once the stress is removed. These materials possess both of the properties exhibiting time-dependent strain. Creep recovery experiment is carried out on the FT, FTP1, and FTP2 (Figure 5b,c,d) gels to inspect the change in viscoelastic property on addition of PEG to the FT

gel. It is manifested from the figures that all the gels exhibit strain recovery property. In the creep phase, a jump of the strain value in response to the applied stress occurs, which is a manifestation of pure elastic nature.³⁷ This is followed by a time-dependent small increase in the strain value at the time interval $t_1 < t < t_2$. After the stress removal, all the gels show strain recovery properties at time $t > t_2$. However, it is very interesting to note that on application of the same amount of stress (0.5 Pa), the FT gel attains a much higher value of strain (0.04) than that of the FTP1 (7.4×10^{-4}) and FTP2 gels (13.6×10^{-4}).

It is also evident from the figure that the FTP1 gel exhibits the highest strain recovery (90%), whereas the FT gel and FTP2 gel exhibits strain recovery of 50% and 68%, respectively, suggesting that FTP1 gel is the most elastic in nature. It may be argued that incorporation of PEG induces sufficient elastic property in the FT gel, though at higher concentration the increase is not so significant, probably due to the onset of self-aggregation of PEG.

Thixotropy is an exceptional viscoelastic property that refers to an isothermal, reversible sol–gel phase transition in which a substance in the gel state is converted to a sol under physical stimuli, such as mechanical shaking or stirring, and returns to the gel state on standing. Nowadays, thixotropic agents are also commercially available and find extensive use in paints, cosmetics, and inks.³⁸ Various detergents, foods, and lubricants also exhibit thixotropy. As a result, the property of thixotropy has attracted enormous attention both from industry and academia. Although there are some reports on thixotropic gels derived from organogelators based on cholesterol derivatives,^{39,40} cyclodextrins,⁴¹ imidazole derivatives,⁴² porphyrin derivatives,⁴³ naphthalenediimide,⁴⁴ dianthracene,⁴⁵ simple

alkyl amides,⁴⁶ and urea,^{47,48} reports on low molecular weight hydrogels exhibiting thixotropic properties are few in the literature.^{49–54} It is interesting to observe that FT gel exhibits thixotropic property (Scheme 1), and for a quantitative evaluation of the thixotropic property we have carried out time sweep experiments under both low strain 0.1% and high strain 100% conditions (Figure 6a).⁵⁴ At the first step, a time

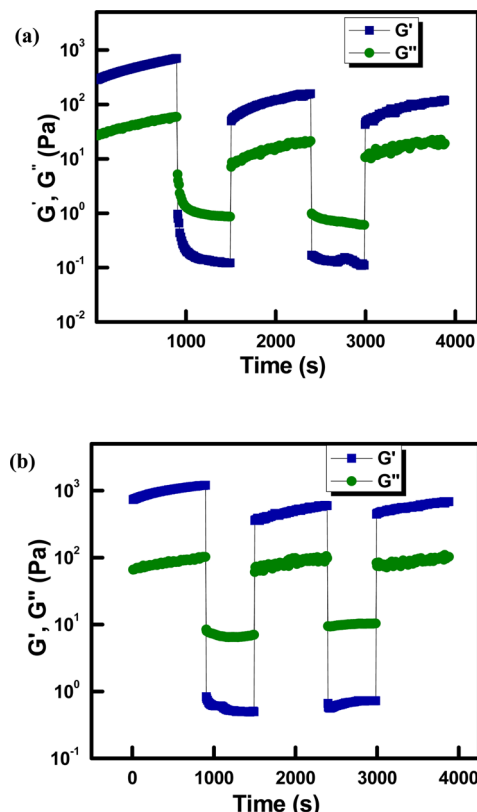


Figure 6. Continuous step strain measurement at alternate 0.1% and 100% strain with time scale for (a) FT gel and (b) FTP2 gel.

sweep experiment is carried out with 0.1% strain, and at the second step the gel is completely destroyed to a quasi-liquid state (sol) by the application of 100% strain as apparent from the modulus values ($G' < G''$). At the third step, recovery of the gel is monitored again with a time sweep experiment under the application of 0.1% of strain, and the modulus values corroborate the reformation of the gel ($G' > G''$). At the fourth step, the gel is again destroyed with 100% strain and is recovered in the fifth step. However, it is noteworthy that the G' value at 0.1% of the strain decreases after each recovery, indicating the FT gel has some hysteresis behavior characteristics of first order phase transition in sol to gel state. We have also investigated whether the thixotropic property of FT gel remains intact after addition of PEG. Figure 6b and Figure S4 portray the thixotropic experiments performed on the FTP2 and FTP1 gels, respectively, and it is obvious that both the gels exhibit thixotropy. The thixotropic behaviors of the FT, FTP1, and FTP2 gels are compared on the basis of time evolution of the storage modulus during the first recovery at 0.1% strain after the gels were destroyed by applying 100% strain, and it is presented in Figure 7. The slope values of the best fitted curves in Figure 7 are 0.11, 0.15, and 0.28 for the FT, FTP1, and FTP2 gel, respectively, unambiguously indicating that the thixotropic behavior is amplified in the order FT gel < FTP1

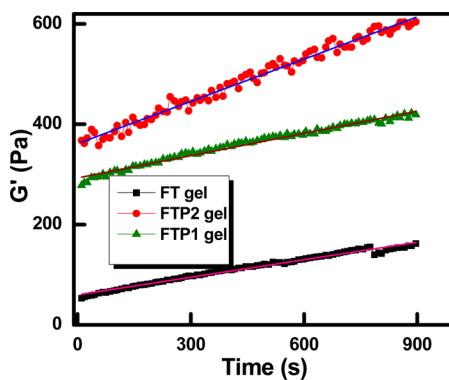
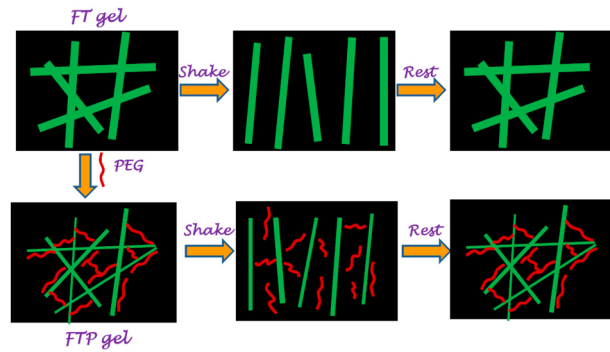


Figure 7. Time dependent evolution of G' values of the gels during recovery under 0.1% strain.

gel < FTP2 gel. This is an interesting new observation of improving the thixotropic property of a hydrogel by incorporation of a polymer. A probable explanation on the enhancement of thixotropic property on addition of PEG is illustrated below. The long fibers produced by the self-assembly of the gelator are interconnected by some junction points or active ends, creating the entangled three-dimensional networks that are competent enough to entrap a large amount of water molecules producing the gels. Application of an external mechanical force ruptures these junction points, separating the fibers from the network, causing the gels to break. Due to the presence of strong supramolecular interactions, the network is regenerated after removing the mechanical force helping in reincarnation of the gel. The thixotropic property is observed in all the gels due to easy self-assembling property of the fibers for the presence of strong H-bonding groups helping the three-dimensional network formation required for gelation. However, in the FTP hybrid gels, PEG behaves like an additional *molecular adhesive*, thereby promoting additional connectors to the gel fibers by supramolecular interactions, hence bringing back the network structure easily. The active ends of the fibers, disintegrated by mechanical force, are brought together by PEG chains in a more accelerated rate than that of FT gel through the supramolecular interaction of hydroxyl groups of PEG chains, causing a faster recovery (Scheme 3).

The choice of a specific PEG molecular weight sample is a crucial part, and here we choose PEG-4000 for this purpose. We have not chosen the higher molecular weight PEG samples because the longer chain PEG would have more entangled,

Scheme 3. Schematic Representation of the Thixotropic Property of FT Gel and Its Improvement by Addition of PEG



coiled and knot structures prohibiting it from acting as a good molecular adhesive to the FT fibers because for steric reasons. Also the lesser amount of interacting OH groups present in the longer PEG chains of the same concentration would impart lesser H-bonding force to interact with the FT fiber. The lower molecular weight of PEG, though it may act as a good molecular adhesive due to higher H-bonding force, would not impart good mechanical property to the gel. Hence we chose an intermediate molecular weight PEG sample to facilitate good molecular adhesive property, imparting better mechanical property to the hybrid gels.

Photophysical Properties. The aggregation behavior of FT is delineated from a comparison of UV-vis spectra of FT solution (0.05%) in dimethyl sulfoxide (DMSO) and in water (pH 7) (Figure 8a). FT remains in the nonaggregated state in

DMSO and the UV-vis spectra of FT solution exhibits peaks at 268 and 290 nm ascribed to the $\pi-\pi^*$ transition of Fmoc and indole chromophoric moieties, respectively.^{55,56} Both these peaks are blue-shifted to 265 and 288 nm, respectively, in aqueous medium (pH 7), indicating stabilization of the π electrons due to aggregation of FT in water. Concentration-dependent UV-vis spectra of FT solution in aqueous medium (pH 7) (Figure S5) indicate that with increasing concentration, the absorbance of both peaks increase in accordance with the Lambert-Beer law.

The fluorescence property of FT solution at a concentration of 0.1% (w/v) and FT gel produced at 0.2% (w/v) concentration are presented in Figure 8b. When excited with a wavelength of 265 nm FT solution exhibit an emission maxima at 400 nm. However, the FT gel exhibits an emission maxima at 395 nm with a 5-fold increase of fluorescence intensity from the sol state. This phenomenon of increase in fluorescence intensity with concentration is termed “aggregation induced emission” (AIE)⁵⁷ and is contrary to the quenching of fluorescence with aggregation commonly called as “concentration quenching” or “aggregation-caused quenching” (ACQ),⁵⁸ which occurs for increased excimers/exciplexes formation at higher concentrations. To establish the occurrence of AIE in our system, we performed fluorescence studies with different concentration of the gelator (Figure 9a), and the fluorescence intensity increases with increasing gelator concentration (0.1% to 0.9%); after that a small decrease of fluorescence intensity is observed. A probable reason for this type of AIE behavior is delineated here. The fluorescence property of FT arises from both the Fmoc and indole chromophores. The energy minimized structure of FT (obtained from Chem3D MM2 level molecular modeling, Figure S6) depicts that the molecule is nonplanar, and in solution phase the free rotation of both the Fmoc and indole moieties can take place. This type of dynamic intermolecular rotation causes the nonradiative decay of the excitons with the solvent molecules, making the molecule nonfluorescent in the solution state.^{58,59} However, gelation bestows planarity to the system by H-bonding and $\pi-\pi$ stacking interactions and stops the intermolecular rotations due to induction of rigidity. Thus, the nonradiative decay paths with the solvent molecules become impeded, causing an increase of fluorescence intensity. To support the proposition, a temperature-dependent fluorescence study of the FT gel at a concentration of 0.4% (w/v) is performed (Figure S7a, b). The fluorescence intensity is plotted against temperature (Figure S7b), and the intensity decreases

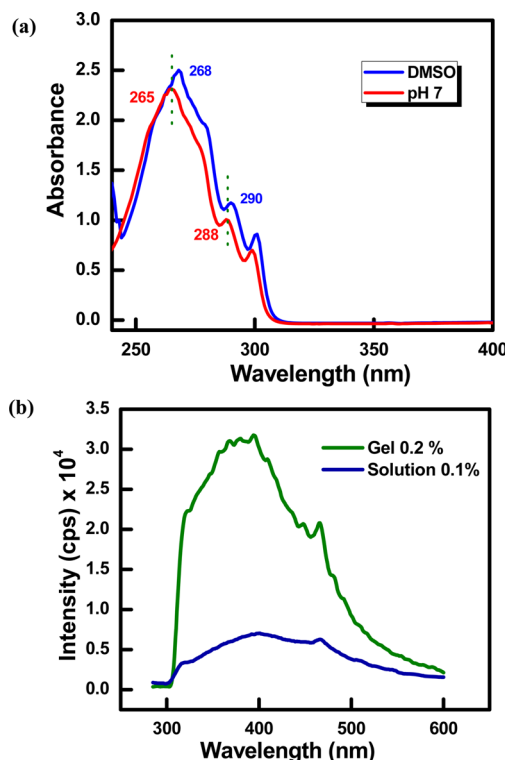


Figure 8. (a) UV-vis spectra of FT (0.05% w/v) in DMSO and in water at pH 7. (b) Fluorescence spectra of FT sol (0.1% w/v) in water and FT hydrogel (0.2% w/v) for excitation at 265 nm.

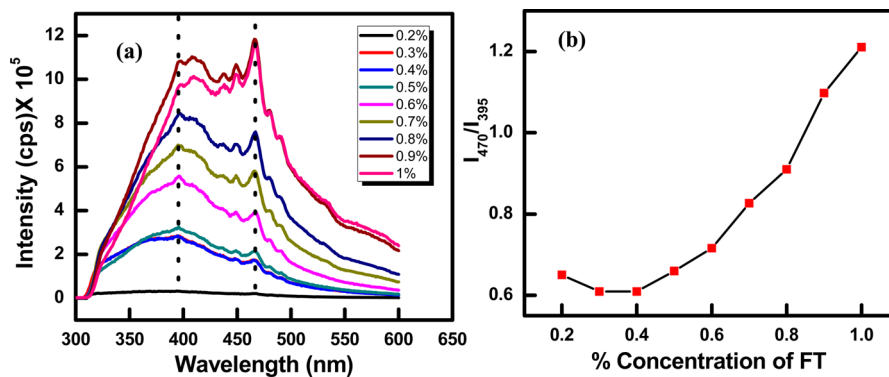


Figure 9. (a) Fluorescence spectra of FT gel at different concentrations for excitation at 265 nm. (b) Plot of ratio of fluorescence intensities at wavelengths 395 and 470 nm with percent concentration of FT.

with increase of temperature up to ~ 50 °C, and above that it remains almost invariant. It is well-known that the molecular rotation is slow at lower temperature, causing higher fluorescence intensities. As the temperature gradually increases, the molecular rotations simultaneously increase, causing lower fluorescence intensities. The sharp fall in the intensity value above 40 °C may be due to the inception of gel breaking.

Another very interesting observation is the ratio of fluorescence intensities at wavelengths 395 and 470 nm. We have calculated the I_{470}/I_{395} values and plotted them against the percent concentration of FT (Figure 9b) in the gel state. It is evident from the figure that the I_{470}/I_{395} value increases after a 0.4% (w/v) concentration of FT, and after a concentration of 0.85%, the ratio is higher than 1. A probable reason for this observation may be obtained from the origin of the two peaks. The peak at 395 nm originates from the tryptophan chromophore,⁶⁰ and the peak at 470 nm occurs due to extended stacking of Fmoc chromophores stabilized by π -stacking interactions.⁶¹ The tryptophan moiety is more hydrophilic than that of Fmoc moiety, disposing the former at the surface of the fibers to facilitate better interactions with the water molecules surrounding the fibers. With increasing FT concentration, the Fmoc chromophores tend to stack more extensively by $\pi-\pi$ interactions producing a better hydrophobic core, decreasing the quenching of excitons with the water molecules, which in turn increase the peak intensity at 470 nm. However, due to solvent quenching with the water molecules, the intensity of the tryptophan moiety at 395 nm does not increase to that extent, though there is comparable enhancement of π -stacking. This is the possible reason for the increase in I_{470}/I_{395} values with FT concentration in the FT gels. Thus, the fluorescence spectra support the model (Scheme 2), which describes the higher possibility of the polar tryptophan molecule to remain at the surface of the fibers.

The fluorescence property of the FT gel is affected by addition of PEG (Figure S8), and there is a small increase in the fluorescence intensity value (~ 1.3 times) after addition of 2 mg of PEG. Here PEG acts as a molecular adhesive to the gel fibers, causing restrictions to the molecular rotations and hence causing a small increase in fluorescence intensity value. With increase of PEG concentration above 2 mg/2 mL of FT gel, the fluorescence intensity decreases, and a possible reason is the self-aggregation of PEG chains making the FT gel fibers free to rotate and hence facilitating the quenching of excitons.

Tunable Drug Release. One of the most wonderful advantages of a thixotropic hydrogel is its injectable nature. Injectable hydrogels can be converted into free-flowing solution by mechanical shaking, and they may be injected using a fine needle as a low viscosity liquid. Owing to the thixotropic property, this free-flowing solution may regain *in vivo* its hydrogel nature. Due to the thixotropic nature of the hydrogels, different water-soluble drugs can be easily encapsulated in the gel matrix at room temperature, avoiding the heating–cooling process, which can substantially diminish the drug's biological activity. These versatile advantages of thixotropic supramolecular hydrogels have made them potential candidates for biological applications.^{62–65} Doxorubicin (DOX) is an effective anticancer drug and is widely used in the treatment of various types of cancers including hematological malignancies, many types of carcinoma (solid tumors), and soft tissue sarcomas.⁶⁶ Here, we have successfully encapsulated DOX in the FT gel matrices exploiting the thixotropic property of the hydrogels under physiological conditions. The DOX loading content is

calculated to be 1.48, 1.32, and 1.19% (w/v) for FT, FTP1, and FTP2 gels, respectively. We have shown a sustained release of DOX from FT gel under physiological conditions and also tuned the release of DOX with the hybrid hydrogels produced from different concentrations of PEG. The release of DOX from the encapsulated state of the FT and FTP hydrogels is investigated from UV–vis spectra by monitoring the absorbance values of DOX at 490 nm at different time intervals. It is evident from Figure 10 that the release of DOX is

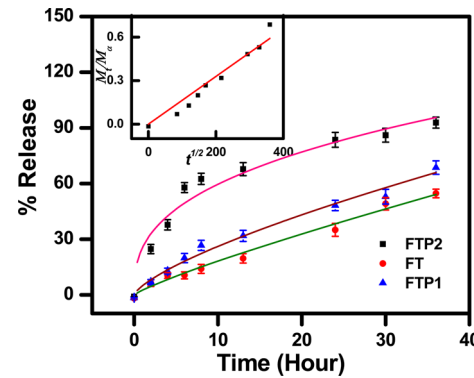


Figure 10. Release profile plot of doxorubicin from FT-DOX, FTP1-DOX, and FTP2-DOX hydrogels (inset: plot of (M_t/M_a) vs $t^{1/2}$ for the FTP1-DOX gel).

linear with increase of time for FT gel, but in FTP1 gel at the initial stage, a slightly sigmoidal release is observed. In FTP2 gel, initially a steeper sigmoidal release than that of FTP1 followed by a linear release is noticed. It is interesting to note that with the increase of PEG concentration in the FTP hybrid gels, the release rate of the drug increases, though there is a loss of sustainable release to some extent. From the release data (Figure 10), the percent release is calculated to be 55%, 69% and 93% for the FT-DOX, FTP1-DOX, and FTP2-DOX hydrogels, respectively, after 36 h of experiment. We have also calculated the value of diffusion coefficient of DOX based on the nonsteady state diffusion model equation³¹

$$(M_t/M_a) = 4(Dt/\pi\lambda^2)^{1/2}$$

where M_t is the total amount of drug released during the measurement, M_a is the total amount of drug loaded within the gel matrix, λ is the thickness of the hydrogel, t is the time (in sec) of the measurement, and D is the diffusion coefficient of the drug molecule. (M_t/M_a) is plotted against $t^{1/2}$ to obtain a linear plot, and from the slope value the diffusion coefficient for the release of DOX from the hydrogels has been computed (inset of Figure 10: (M_t/M_a) vs $t^{1/2}$ plot for the FTP1-DOX gel). The diffusion coefficient values are 4.2×10^{-11} , 1.1×10^{-10} , and $3.7 \times 10^{-10} \text{ m}^2\text{s}^{-1}$ for the FT-DOX, FTP1-DOX, and FTP2-DOX hydrogels, respectively. It is very interesting that with increase in PEG concentration in the FTP hydrogels, the percent release along with the diffusion coefficient of DOX increases. To shed light on the above observation, we have studied the FTIR spectra of the dried FT-DOX, FTP1-DOX, and FTP2-DOX hydrogels (Figure 11). It is evident from the figure that the carbonyl stretching frequency of FT in the FT xerogel (1676 cm^{-1}) shifts to a lower position in the FT-DOX gel (1672 cm^{-1}), suggesting H-bonding interactions between DOX and FT molecules. However, in the FTP1-DOX and FTP2-DOX xerogels, the carbonyl stretching frequencies shift

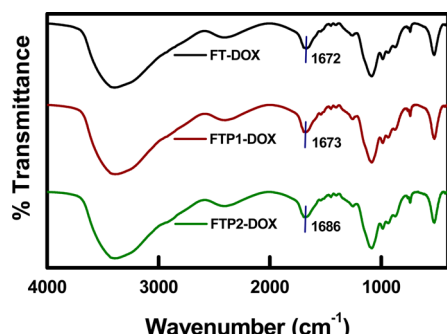
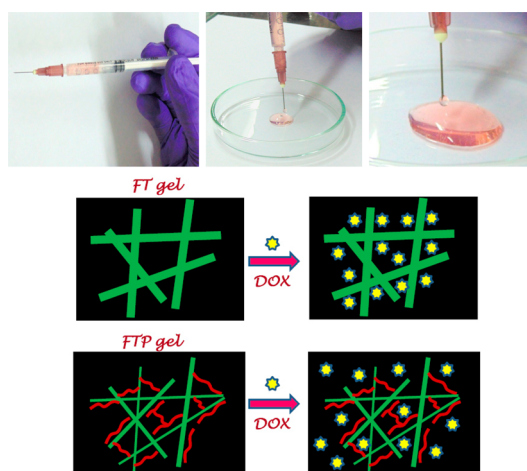


Figure 11. FTIR spectra of dried FT-DOX, FTP1-DOX, and FTP2-DOX hydrogels.

to higher positions at 1673 cm^{-1} and at 1686 cm^{-1} for **FTP1-DOX** and **FTP2-DOX** xerogels, respectively. It indicates weakening of H-bonding interactions between DOX and FT due to integration of PEG in the gels. The PEG chains present in the **FTP1-DOX** and **FTP2-DOX** gels may occupy the H-bonding sites of the FT molecules, thereby making it difficult for the DOX molecules to interact with FT. Thus, the FT gel entraps the drug molecule more efficiently than the FTP gels (Scheme 4) and so the release of DOX increases in the order

Scheme 4. Injectable Nature of the FT-DOX Hydrogel and Schematic Representation of Entrapment of DOX in the FT and FTP Hydrogels



FT-DOX < FTP1-DOX < FTP2-DOX. So, here we have successfully encapsulated DOX in the gel matrices and also showed its sustained release under physiological conditions ($\text{pH } 7$ and temperature $37\text{ }^\circ\text{C}$). Moreover, we have also successfully tuned both the release rate (diffusion coefficient) and final release of DOX by incorporating an appropriate amount of PEG in the gel matrices. To, our knowledge, this tuning of release of a drug using a biocompatible polymer in a supramolecular thixotropic gel system is reported here for the first time. Also the DOX-loaded hydrogels are injectable in nature, which is elegantly portrayed in Scheme 4. Owing to their injectable nature, the hydrogels can behave as an effective *in vivo* drug carrier.

CONCLUSION

Stimuli responsive supramolecular gels are advantageous in many aspects, but their poor mechanical properties limit their

large scale application as functional materials. Fmoc-L-tryptophan (FT) produces gel in $\text{pH } 7$ buffer at a minimum gelation concentration of 0.2% (w/v). FTIR and WAXS patterns indicate the presence of hydrogen bonding and π stacking in the gels. To improve the mechanical property of the gels, PEG is added into the gel matrix, and the hybrid FTP gels have supramolecular interactions between FT and PEG. Both the FT and FTP gels exhibit fibrous morphology, but on addition of 1 mg PEG to the FT gel, a $\sim 28\text{ nm}$ decrease in the diameter values occurs. Increment of the storage and loss modulus is observed for the FTP gels relative to the FT gel with the highest increase (2815%) of the former for **FTP2.5** gel. The complex modulus initially increases with addition of PEG in the FT gel, showing maximum increase of 2811% for **FTP2.5** gel, and then decreases. The decrease of G^* at higher concentrations of PEG ($>2.5\text{ mg}$) may be attributed to the increased self-aggregation between the PEG chains rather than forming assembly with FT fibers. Non-Newtonian viscosity is observed for all the gels, and critical shear rate values are 100 S^{-1} , 126 S^{-1} and 159 S^{-1} for the FT, **FTP1** and **FTP2** gels, respectively. The **FTP1** gel exhibits highest strain recovery (90%), whereas the FT gel and **FTP2** gel exhibit strain recoveries of 50% and 68%, respectively. All the FT, **FTP1**, and **FTP2** gels are thixotropic in nature, and thixotropy increases in the order $\text{FT} < \text{FTP1} < \text{FTP2}$ gels. The UV-vis spectra of FT gel exhibit a blue shift in the $\pi-\pi^*$ transition peaks relative to that of the FT solution, and the gel shows 5-fold increase in fluorescence intensity compared to that from the solution due to “aggregation induced emission.” A small increase in fluorescence intensity is observed after addition of 2 mg PEG in the FT gel, but at higher PEG concentration quenching occurs. Exploiting the thixotropic property of the FT and FTP hybrid gels, we have successfully encapsulated DOX, and we have shown a tunable release of DOX by incorporating the appropriate amount of PEG in the gel matrices under physiological conditions. Both FT and PEG are biocompatible, and the hydrogels are injectable, so the system may find application for *in vivo* drug delivery at a tunable rate.

ASSOCIATED CONTENT

S Supporting Information

Table of rheological data, digital images of gels, WAXS data, TEM images, rheological data, UV-vis spectra, energy minimized structure, and fluorescence data. The Supporting Information is available free of charge on the ACS Publications website at DOI: 10.1021/acs.jpcb.5b02424.

AUTHOR INFORMATION

Corresponding Author

*Address: Polymer Science Unit, Indian Association for the Cultivation of Science, Jadavpur Kolkata-700 032, INDIA. Telephone No. 913324734971; e-mail: psuakn@iacs.res.in.

Notes

The authors declare no competing financial interest.

ACKNOWLEDGMENTS

P.C., S.M., and P.B. acknowledge CSIR, New Delhi for providing the fellowship. The instrumental facility availed from DST sponsored “Unit of Nanoscience at IACS” project is gratefully acknowledged.

■ REFERENCES

- (1) Weiss, R. G.; Terech, P. *Molecular Gels: Materials with Self-Assembled Fibrillar Network*; Springer: Dordrecht, 2006.
- (2) Estroff, L. A.; Hamilton, A. D. Water Gelation by Small Organic Molecules. *Chem. Rev.* **2004**, *104*, 1201–1218.
- (3) Babu, S. S.; Praveen, V. K.; Ajayaghosh, A. Functional π -Gelators and Their Applications. *Chem. Rev.* **2014**, *114*, 1973–2129.
- (4) Banerjee, S.; Das, R. K.; Maitra, U. Supramolecular Gels ‘in Action’. *J. Mater. Chem.* **2009**, *19*, 6649–6687.
- (5) Dong, S.; Luo, Y.; Yan, X.; Zheng, B.; Ding, X.; Yu, Y.; Ma, Z.; Zhao, Q.; Huang, F. A Dual-Responsive Supramolecular Polymer Gel Formed by Crown Ether Based Molecular Recognition. *Angew. Chem., Int. Ed.* **2011**, *50*, 1905–1909.
- (6) Zhang, M.; Xu, D.; Yan, X.; Chen, J.; Dong, S.; Zheng, B.; Huang, F. Self-Healing Supramolecular Gels Formed by Crown Ether Based Host–Guest Interactions. *Angew. Chem., Int. Ed.* **2012**, *51*, 7011–7015.
- (7) Yan, X.; Xu, D.; Chi, X.; Chen, J.; Dong, S.; Ding, X.; Yu, Y.; Huang, F. A Multiresponsive, Shape-Persistent, and Elastic Supramolecular Polymer Network Gel Constructed by Orthogonal Self-Assembly. *Adv. Mater.* **2012**, *24*, 362–369.
- (8) Dong, S.; Zheng, B.; Xu, D.; Yan, X.; Zhang, M.; Huang, F. A Crown Ether Appended Super Gelator with Multiple Stimulus Responsiveness. *Adv. Mater.* **2012**, *24*, 3191–3195.
- (9) Liu, X. Y.; Sawant, P. D. Micro/Nanoengineering of the Self-Organized Three-Dimensional Fibrous Structure of Functional Materials. *Angew. Chem., Int. Ed.* **2002**, *41*, 3641–3645.
- (10) Liu, X. Y.; Sawant, P. D.; Tan, W. B.; Noor, I. B. M.; Pramesti, C.; Chen, B. H. Creating New Supramolecular Materials by Architecture of Three-Dimensional Nanocrystal Fiber Networks. *J. Am. Chem. Soc.* **2002**, *124*, 15055–15063.
- (11) Wang, R.; Liu, X. Y.; Xiong, J.; Li, J. Real-Time Observation of Fiber Network Formation in Molecular Organogel: Supersaturation-Dependent Microstructure and Its Related Rheological Property. *J. Phys. Chem. B* **2006**, *110*, 7275–7280.
- (12) Huang, X.; Terech, P.; Raghavan, S. R.; Weiss, R. G. Kinetics of α -Cholestan-3 β -yl N-(2-Naphthyl)carbamate/n-Alkane Organogel Formation and Its Influence on the Fibrillar Networks. *J. Am. Chem. Soc.* **2005**, *127*, 4336–4344.
- (13) Li, J. L.; Liu, X. Y.; Strom, C. S.; Xiong, J. Y. Engineering of Small Molecule Organogels by Design of the Nanometer Structure of Fiber Networks. *Adv. Mater.* **2006**, *18*, 2574–2578.
- (14) Jhaveri, S. J.; McMullen, J. D.; Sijbesma, R.; Tan, L.-S.; Zipfel, W.; Ober, C. K. Direct Three-Dimensional Microfabrication of Hydrogels via Two-Photon Lithography in Aqueous Solution. *Chem. Mater.* **2009**, *21*, 2003–2006.
- (15) Friggeri, A.; Feringa, B. L.; van Esch, J. Entrapment and Release of Quinoline Derivatives Using A Hydrogel of A Low Molecular Weight Gelator. *J. Controlled Release* **2004**, *97*, 241–248.
- (16) Tiller, J. C. Increasing the Local Concentration of Drugs by Hydrogel Formation. *Angew. Chem., Int. Ed.* **2003**, *42*, 3072–3075.
- (17) Liu, D.-L.; Chang, X.; Dong, C.-M. Reduction- and Thermo-Sensitive Star Poly peptide Micelles and Hydrogels for On-Demand Drug Delivery. *Chem. Commun.* **2013**, *49*, 1229–1231.
- (18) Kiyonaka, S.; Sugiyasu, K.; Shinkai, S.; Hamachi, I. First Thermally Responsive Supramolecular Polymer Based on Glycosylated Amino Acid. *J. Am. Chem. Soc.* **2002**, *124*, 10954–10955.
- (19) Adhikari, B.; Palui, G.; Banerjee, A. Self-Assembling Tripeptide Based Hydrogels and Their Use in Removal of Dyes from Waste-Water. *Soft Matter* **2009**, *5*, 3452–3460.
- (20) Chakraborty, P.; Roy, B.; Bairi, P.; Nandi, A. K. Improved Mechanical and Photophysical Properties of Chitosan Incorporated Folic Acid Gel Possessing The Characteristics of Dye and Metal Ion Absorption. *J. Mater. Chem.* **2012**, *22*, 20291–20298.
- (21) Vemula, P. K.; John, G. Smart Amphiphiles: Hydro/Organogelators for *In Situ* Reduction of Gold. *Chem. Commun.* **2006**, 2218–2220.
- (22) Lee, K. Y.; Mooney, D. J. Hydrogels for Tissue Engineering. *Chem. Rev.* **2001**, *101*, 1869–1880.
- (23) Ellis-Behnke, R. G.; Liang, Y.-X.; You, S.-W.; Tay, D. K. C.; Zhang, S.; So, K.-F.; Schneider, G. E. Nano Neuro Knitting: Peptide Nanofiber Scaffold for Brain Repair and Axon Regeneration With Functional Return of Vision. *Proc. Natl. Acad. Sci. U. S. A.* **2006**, *103*, 5054–5059.
- (24) Wang, X.; Horii, A.; Zhang, S. Designer Functionalized Self-Assembling Peptide Nanofiber Scaffolds For Growth, Migration, and Tubulogenesis of Human Umbilical Vein Endothelial Cells. *Soft Matter* **2008**, *4*, 2388–2395.
- (25) Kiyonaka, S.; Sada, K.; Yoshimura, I.; Shinkai, S.; Kato, N.; Hamachi, I. Semi-Wet Peptide/Protein Array Using Supramolecular Hydrogel. *Nat. Mater.* **2004**, *3*, 58–64.
- (26) Cornwell, D. J.; Okesola, B. O.; Smith, D. K. Hybrid Polymer and Low Molecular Weight Gels – Dynamic Two-Component Soft Materials with both Responsive and Robust Nanoscale Networks. *Soft Matter* **2013**, *9*, 8730–8736.
- (27) Cornwell, D. J.; Okesola, B. O.; Smith, D. K. Multidomain Hybrid Hydrogels: Spatially Resolved Photopatterned Synthetic Nanomaterials Combining Polymer and Low-Molecular-Weight Gelators. *Angew. Chem., Int. Ed.* **2014**, *53*, 12461–12465.
- (28) Wang, Q.; Yang, Z.; Wang, L.; Ma, M.; Xu, B. Molecular Hydrogel-Immobilized Enzymes Exhibit Superactivity and High Stability in Organic Solvents. *Chem. Commun.* **2007**, 1032–1034.
- (29) Zhang, Y.; Gu, H.; Yang, Z.; Xu, B. Supramolecular Hydrogels Respond to Ligand-Receptor Interaction. *J. Am. Chem. Soc.* **2003**, *125*, 13680–13681.
- (30) Yang, Z.; Xu, K.; Wang, L.; Gu, H.; Wei, H.; Zhang, M.; Xu, B. Self-Assembly of Small Molecules Affords Multifunctional Supramolecular Hydrogels for Topically Treating Simulated Uranium Wounds. *Chem. Commun.* **2005**, 4414–4416.
- (31) Mahler, A.; Reches, M.; Rechter, M.; Cohen, S.; Gazit, E. Rigid, Self-Assembled Hydrogel Composed of a Modified Aromatic Dipeptide. *Adv. Mater.* **2006**, *18*, 1365–1370.
- (32) Roy, S.; Banerjee, A. Amino Acid Based Smart Hydrogel: Formation, Characterization and Fluorescence Properties of Silver Nanoclusters within the Hydrogel Matrix. *Soft Matter* **2011**, *7*, 5300–5308.
- (33) Bairi, P.; Roy, B.; Routh, P.; Sen, K.; Nandi, A. K. Self-Sustaining, Fluorescent and Semi-Conducting Co-Assembled Organogel of Fmoc Protected Phenylalanine with Aromatic Amines. *Soft Matter* **2012**, *8*, 7436–7445.
- (34) Palui, G.; Banerjee, A. Fluorescent Gel from a Self-Assembling New Chromophoric Moiety Containing Azobenzene Based Tetraamide. *J. Phys. Chem. B* **2008**, *112*, 10107–10115.
- (35) Li, F.; Zhu, Y.; You, B.; Zhao, D.; Ruan, Q.; Zeng, Y.; Ding, C. Smart Hydrogels Co-switched by Hydrogen Bonds and π - π Stacking for Continuously Regulated Controlled-Release System. *Adv. Funct. Mater.* **2010**, *20*, 669–676.
- (36) Keith, H. D.; Padden, F. J. A Phenomenological Theory of Spherulitic Crystallization. *J. Appl. Phys.* **1963**, *34*, 2409–2421.
- (37) Yan, C.; Pochan, D. J. Rheological Properties of Peptide-Based Hydrogels for Biomedical and Other Applications. *Chem. Soc. Rev.* **2010**, *39*, 3528–3540.
- (38) Barnes, H. A. Thixotropy—A Review. *J. Non-Newtonian Fluid Mech.* **1997**, *70*, 1–33.
- (39) Xue, M.; Gao, D.; Liu, K.; Peng, J.; Fang, Y. Cholesteryl Derivatives as Phase-Selective Gelators at Room Temperature. *Tetrahedron* **2009**, *65*, 3369–3377.
- (40) Huang, X.; Raghavan, S. R.; Terech, P.; Weiss, R. G. Distinct Kinetic Pathways Generate Organogel Networks with Contrasting Fractality and Thixotropic Properties. *J. Am. Chem. Soc.* **2006**, *128*, 15341–15352.
- (41) Araki, J.; Ito, K. Strongly Thixotropic Viscosity Behavior of Dimethylsulfoxide Solution of Polyrotaxane Comprising a-Cyclodextrin and Low Molecular Weight Poly(ethylene glycol). *Polymer* **2007**, *48*, 7139–7144.
- (42) Weng, W.; Jamieson, A. M.; Rowan, S. J. Structural Origin of the Thixotropic Behavior of A Class of Metallosupramolecular Gels. *Tetrahedron* **2007**, *63*, 7419–7431.

- (43) Shirakawa, M.; Fujita, N.; Shinkai, S. A Stable Single Piece of Unimolecularly π -Stacked Porphyrin Aggregate in a Thixotropic Low Molecular Weight Gel: A One-Dimensional Molecular Template for Polydiacetylene Wiring up to Several Tens of Micrometers in Length. *J. Am. Chem. Soc.* **2005**, *127*, 4164–4165.
- (44) Dawn, A.; Shiraki, T.; Ichikawa, H.; Takada, A.; Takahashi, Y.; Tsuchiya, Y.; Lien, L. T. N.; Shinkai, S. Stereochemistry-Dependent, Mechanoresponsive Supramolecular Host Assemblies for Fullerenes: A Guest-Induced Enhancement of Thixotropy. *J. Am. Chem. Soc.* **2012**, *134*, 2161–2171.
- (45) Mukhopadhyay, P.; Fujita, N.; Takada, A.; Kishida, T.; Shirakawa, M.; Shinkai, S. Regulation of a Real-Time Self-Healing Process in Organogel Tissues by Molecular Adhesives. *Angew. Chem. Int. Ed.* **2010**, *49*, 6338–6342.
- (46) Lescanne, M.; Grondin, P.; d'Aléo, A.; Fages, F.; Pozzo, J.-L.; Monval, O. M.; Reinheimer, P.; Colin, A. Thixotropic Organogels Based on a Simple N-Hydroxyalkyl Amide: Rheological and Aging Properties. *Langmuir* **2004**, *20*, 3032–3041.
- (47) Brinksma, J.; Feringa, B. L.; Kellogg, R. M.; Vreeker, R.; van Esch, J. Rheology and Thermotropic Properties of Bis-Urea-Based Organogels in Various Primary Alcohols. *Langmuir* **2000**, *16*, 9249–9255.
- (48) van Esch, J.; Schoonbeek, F.; de Loos, M.; Kooijman, H.; Spek, A. L.; Kellogg, R. M.; Feringa, B. L. Cyclic Bis-Urea Compounds as Gelators for Organic Solvents. *Chem.—Eur. J.* **1999**, *5*, 937–950.
- (49) Ma, D.; Zhang, L.-M. Supramolecular Gelation of a Polymeric Prodrug for Its Encapsulation and Sustained Release. *Biomacromolecules* **2011**, *12*, 3124–3130.
- (50) Freunlich, H. *Thixotropie*; Hermann: Paris, 1935.
- (51) Pakhomov, P.; Khizhnyak, S.; Ovchinnikov, M.; Komarov, P. Supramolecular Hydrogels Based on Silver Mercaptide. Self-Organization and Practical Application. *Macromol. Symp.* **2012**, *316*, 97–107.
- (52) Sakka, S.; Kozuka, H. Rheology of Sols and Fibre Drawing. *J. Non-Cryst. Solids* **1988**, *100*, 142–153.
- (53) Roy, B.; Bairi, P.; Chakraborty, P.; Nandi, A. K. Stimuli-Responsive, Thixotropic Bicomponent Hydrogel of Melamine-Zn(II)-Orotate Complex. *Supramol. Chem.* **2013**, *25*, 335–343.
- (54) Bairi, P.; Chakraborty, P.; Mondal, S.; Roy, B.; Nandi, A. K. A Thixotropic Supramolecular Hydrogel of Adenine and Riboflavin-5'-Phosphate Sodium Salt Showing Enhanced Fluorescence Properties. *Soft Matter* **2014**, *10*, 5114–5120.
- (55) Li, Y.; Cousins, B. G.; Ulijn, R. V.; Kinloch, I. A. A Study of the Dynamic Interaction of Surfactants with Graphite and Carbon Nanotubes using Fmoc-Amino Acids as a Model System. *Langmuir* **2009**, *25*, 11760–11767.
- (56) Edelhoch, H. Spectroscopic Determination of Tryptophan and Tyrosine in Proteins. *Biochemistry* **1967**, *6*, 1948–1954.
- (57) Luo, J.; Xie, Z.; Lam, J. W. Y.; Cheng, L.; Chen, H.; Qiu, C.; Kwok, H. S.; Zhan, X.; Liu, Y.; Zhu, D.; Tang, B. Z. Aggregation-Induced Emission of 1-Methyl-1,2,3,4,5-Pentaphenylsilole. *Chem. Commun.* **2001**, 1740–1741.
- (58) Hong, Y.; Lam, J. W. Y.; Tang, B. Z. Aggregation-Induced Emission. *Chem. Soc. Rev.* **2011**, *40*, 5361–5388.
- (59) Chen, Y.; Lv, Y.; Han, Y.; Zhu, B.; Zhang, F.; Bo, Z.; Liu, C.-Y. Dendritic Effect on Supramolecular Self-Assembly: Organogels with Strong Fluorescence Emission Induced by Aggregation. *Langmuir* **2009**, *25*, 8548–8555.
- (60) Vivian, J. T.; Callis, P. R. Mechanisms of Tryptophan Fluorescence Shifts in Proteins. *Biophys. J.* **2001**, *80*, 2093–2109.
- (61) Hughes, M.; Birchall, L. S.; Zuberi, K.; Aitken, L. A.; Debnath, S.; Javid, N.; Ulijn, R. V. Differential Supramolecular Organisation of Fmoc-dipeptides with Hydrophilic Terminal Amino Acid Residues by Biocatalytic Self-Assembly. *Soft Matter* **2012**, *8*, 11565–11574.
- (62) Pek, Y. S.; Wan, A. C. A.; Shekaran, A.; Zhuo, L.; Ying, J. Y. A Thixotropic Nanocomposite Gel for Three-Dimensional Cell Culture. *Nat. Nanotechnol.* **2008**, *3*, 671–675.
- (63) Wang, H.; Wang, Z.; Yi, X.; Long, J.; Liu, J.; Yang, Z. Anti-Degradation of a Recombinant Complex Protein by Incorporation in Small Molecular Hydrogels. *Chem. Commun.* **2011**, *4*, 955–957.
- (64) Yan, C.; Altunbas, A.; Yucel, T.; Nagarkar, R. P.; Schneider, J. P.; Pochan, D. J. Injectable Solid Hydrogel: Mechanism of Shear-Thinning and Immediate Recovery of Injectable β -Hairpin Peptide Hydrogels. *Soft Matter* **2010**, *6*, 5143–5156.
- (65) Ren, C.; Song, Z.; Zheng, W.; Chen, X.; Wang, L.; Kong, D.; Yang, Z. Disulfide Bond as a Cleavable Linker for Molecular Self-Assembly and Hydrogelation. *Chem. Commun.* **2011**, *47*, 1619–1621.
- (66) Tacar, O.; Sriamornsak, P.; Dass, C. R. Doxorubicin: An Update on Anticancer Molecular Action, Toxicity and Novel Drug Delivery Systems. *J. Pharm. Pharmacol.* **2013**, *65*, 157–170.